JOURNAL OF SOLID STATE CHEMISTRY 89, 227–236 (1990)

Structure and Properties of a New Family of Ceramic Phosphides: $AgZnLaP_2$, $AgZnSmP_2$, and $CuZnSmP_2$

PALOMA TEJEDOR AND ANGELICA M. STACY*

Department of Chemistry, University of California, Berkeley, Berkeley, California 94720

Received November 16, 1989; in revised form June 18, 1990

Three new quaternary phosphides, $AgZnLaP_2$, $AgZnSmP_2$, and $CuZnSmP_2$, were synthesized by direct reaction of the elements. Recrystallization by isothermal chemical vapor transport, using iodine as the transporting agent, yielded single crystals. The structure of $AgZnSmP_2$ was refined from single crystal X-ray data in the space group $P\bar{3}m1$ to an R value of 2.11%. The lattice parameters are $a = 4.1247(4)$ Å and $c = 6.6920(6)$ Å. The other two compounds were found to be isostructural, with lattice parameters $a = 4.194(2)$ Å and $c = 6.817(2)$ Å for $AgZnLaP_2$ and $a = 4.016(2)$ Å and $c = 6.592(2)$ Å for $CuZnSmP_2$. These new materials sinter at temperatures near 800°C, have melting points above 1100°C, and do not react with water at room temperature. Diffuse reflectance spectra and the temperature dependence of the resistivity indicate that these materials are heavily doped semiconductors.

Introduction

A need has emerged in recent years for ceramic materials with improved optical properties. In particular, materials which transmit in the infrared are required for high performance infrared detectors. While many ceramic materials are transparent in the visible region of the spectrum, there is a paucity of materials which transmit in the infrared. This is because most ceramic materials contain light elements such as oxygen and boron, and therefore have vibrational excitations in the infrared region. We are exploring the suitability of phosphides for such applications. Unfortunately, although phosphides may not have vibrational excitations in the infrared, many have electronic excitations; most of the transition metal phosphides are metals. Therefore, we chose to study phosphides containing electropositive metals with phosphorus in the formal oxidation state of −3. These are the most likely candidates among the phosphides for infrared windows because they will have the largest band gaps. In the following, we report the synthesis, structure, and properties of three new quaternary phosphides: $AgZnLaP_2$, $AgZnSmP_2$, and $CuZnSmP_2$. The applicability of these materials as infrared transmitting ceramics is examined.

Experimental

Synthesis and Crystal Growth

$AgZnLaP_2$, $AgZnSmP_2$, and $CuZnSmP_2$ were synthesized by direct reaction of stoichiometric amounts of the metallic elements (Cu: Johnson Matthey Inc., 99.999%; Ag: Aldrich Chemical Co., 99.999%; Zn: Aldrich Chemical Co., 99.99%; La: Johnson Matthey Inc., 99.9%; and Sm: Johnson Matthey Inc., 99.9%) and red phosphorus (Johnson Matthey Inc., 99.999%) in sealed quartz

To whom correspondence should be addressed.

0022-4596/90 $3.00

ampoules. The metals were stored and handled exclusively under argon in a Vacuum Atmospheres dry box. The initial amount of phosphorus used was such that the total pressure in the ampoule did not exceed 8 atm P_4 at 1000°C. The ampoules were heated initially to 500°C at 50°C/hr, and soaked at this temperature for about 15 hr. The temperature then was increased at 80°C/hr to a final temperature between 850 and 1000°C, and held at this temperature for 3 to 7 days. Finally, the ampoules were quenched to room temperature in about 10 min. The powders obtained were used subsequently as starting materials for single crystal growth.

Crystal growth was carried out by chemical vapor transport (CVT) of the prereacted material in quartz ampoules. In order to avoid thermal decomposition of the quaternary phase into mixtures of binary phases, the CVT reactions were carried out under isothermal conditions at temperatures between 1000 and 1100°C, for periods of time between 4 and 10 days. Iodine (~100 mg, Mallinckrodt, 99.9%) was used as the transporting agent. It was also possible to obtain single crystals of $CuZnSmP_2$ in a single step by direct reaction of stoichiometric amounts of copper (I) iodide (Aldrich Chemical Co., 99%) with zinc, samarium, and red phosphorus, using the same temperature cycle described above for preparation of powders.

Elemental Analysis

The compositions of single crystals of $AgZnLaP_2$, $AgZnSmP_2$, and $CuZnSmP_2$ were determined by wavelength dispersive X-ray fluorescence analysis, using an ARL SEMQ microprobe with a 52.5° take-off angle. The operating voltage was set at 20 keV, the sample current was adjusted to 30 nA on MgO, and counting times were 10 sec for both standards and samples. Count rates were kept below 10,000 cps to minimize detector dead-time losses.

For quantitative analysis, the intensities of each of the X-ray emissions of the single crystals were compared with those of a standard. Four fixed spectrometers (Si, Fe, Ca, and Al) and four scanning spectrometers allowed for data acquisition of a maximum of eight elements simultaneously. GaP, Ag metal, Zn metal, Cu metal, SmS, and LaF_3 were chosen as standards; the compositions of these standards had been determined previously by wet chemistry. Background counts for the wavelength regions of interest were determined by measuring the background fluorescence of synthetic materials with purities in excess of 99.99%. After correction for the background and interferences, Bence–Albee corrections (*1*), modified to use quadratic coefficients, along with atomic number and backscattering algorithms, were applied to the X-ray counts.

TABLE I

CRYSTAL DATA COLLECTION PARAMETERS FOR $AgZnSmP_2$

Radiation: Mo$K\alpha$ (λ = 0.71073 Å)
Monochromator: Highly oriented graphite (2θ = 12.2°)
Detector: Crystal scintillation counter, with PHA
Reflections measured: ±h, ±k, ±l
2θ range: $2\theta < 55°$
Scan type: $\theta - 2\theta$
Scan width: $\Delta\theta = 0.55 + 0.35 \tan\theta$
Scan speed: 0.66 to 6.70 (θ, °/min)
Background: Measured over 0.25 × $\Delta\theta$ added to each end of the scan

Structure Determination

Precession photos of single crystals of $AgZnLaP_2$, $AgZnSmP_2$, and $CuZnSmP_2$ showed trigonal Laue symmetry for all three materials. Single crystal intensity data were collected for $AgZnSmP_2$ on an Enraf-Nonius CAD-4 diffractometer (*2*). Automatic peak search and indexing procedures yielded a trigonal reduced primitive cell which was used for all further work. The specific data collection parameters are summarized in Table I.

Intensities for 916 reflections were mea-

sured ($\pm h$, $\pm k$, $\pm l$, $2\theta < 55°$) for a crystal with a tabular rhomboidral shape with dimensions 0.08 × 0.17 × 0.32 mm. The raw intensities were converted to structure factor amplitudes and their e.s.d.'s by correction for scan speed, background, and Lorentz and polarization effects (*3*). Inspection of the azimuthal scan data showed a variation $I_{min}/I_{max} = 0.63$ for the average curve. An empirical correction based on the observed variation was applied to the data ($T_{max} = 1.0$, $T_{min} = 0.65$). The Laue symmetry and the lack of systematic absences suggested $P3m1$ and $P\bar{3}m1$ as possible space groups, as well as other lower symmetry groups. The choice of the high-symmetry group $P\bar{3}m1$ was confirmed by the successful solution and refinement of the structure. Averaging the symmetry equivalent data gave 111 unique data in the final data set. The averaging residuals were $R(I) = 2.3\%$, $R(F) = 1.3\%$ for the 632 data included in the averaging, and $R(I) = 5.8\%$, $R(F) = 2.5\%$ for all 916 data. A subset of 276 data were more than 5σ away from their average and were not included in the averaged data set.

The structure was solved by Patterson and trial-and-error methods in the space group $P\bar{3}m1$ and refined via standard least-squares and Fourier techniques. After some difficulty in assigning electron density, and discovery of the disorder of the Ag and Zn atoms, a good residual was achieved. A secondary extinction parameter (*4*) was included in the calculations from an early stage (maximum correction = 24% on F). In the final cycles, four reflections with large weighted differences were removed from the refinement.

The final residuals for 10 variables refined against the 105 accepted data for which $F^2 > 3\sigma(F^2)$ were $R = 2.10\%$, $wR = 2.52\%$, and GOF = 1.012. The R value for all data was 2.11%. The quantity minimized by the least squares program was $\Sigma w(|F_0| - |F_c|)^2$, where w is the weight of a given observation. The p-factor used to reduce the weight of the intense reflections was set to 0.04 in the last cycles of refinement. The analytical forms of the scattering factors for the neutral atoms were used (*5*) and all scattering factors were corrected for both the real and the imaginary components of anomalous dispersion (*6*). Inspection of the residuals ordered in ranges of $\sin\theta/g$, $|F_0|$, and parity and value of the individual indexes showed no unusual features or trends. The largest peak in the final difference Fourier map had an electron density of 0.91 $e^-/Å^3$, and the lowest excursion was -1.68 $e^-/Å$. Both were located near metal atoms.

Powder diffraction data for $AgZnLaP_2$, $AgZnSmP_2$, and $CuZnSmP_2$ were obtained on an 11.46-cm Debye–Scherrer camera. The lines on the diffraction patterns were read to 0.03 mm. Distances and angles were determined by the Straumanis method (*7*), which corrects for film shrinkage and systematic errors derived from the camera geometry. The powder patterns were indexed on the basis of the trigonal Laue symmetry ($P\bar{3}m1$). Lattice constants were refined from the powder data using the method of Cohen's least squares (*8*).

Physical Measurements

The temperature dependences of the electrical resistivities of $AgZnLaP_2$, $AgZnSmP_2$, and $CuZnSmP_2$ were measured on samples prepared by pressing the prereacted phosphides into 1/4-in. diameter pellets at 8000 psi, and subsequently sintering them in quartz ampoules at 800°C for 4 hr. The pellets then were cut to a final size of approximately 4 × 1 × 0.5 mm. Four contacts were made by attaching gold wires with conducting silver paint (duPont Conductor Composition 4929). Electrical resistivities were determined by the four-probe technique using a Keithley 177 DMM microvoltmeter and an AC current source. Currents injected in the samples ranged between 1×10^{-4} and 1×10^{-3} A. A

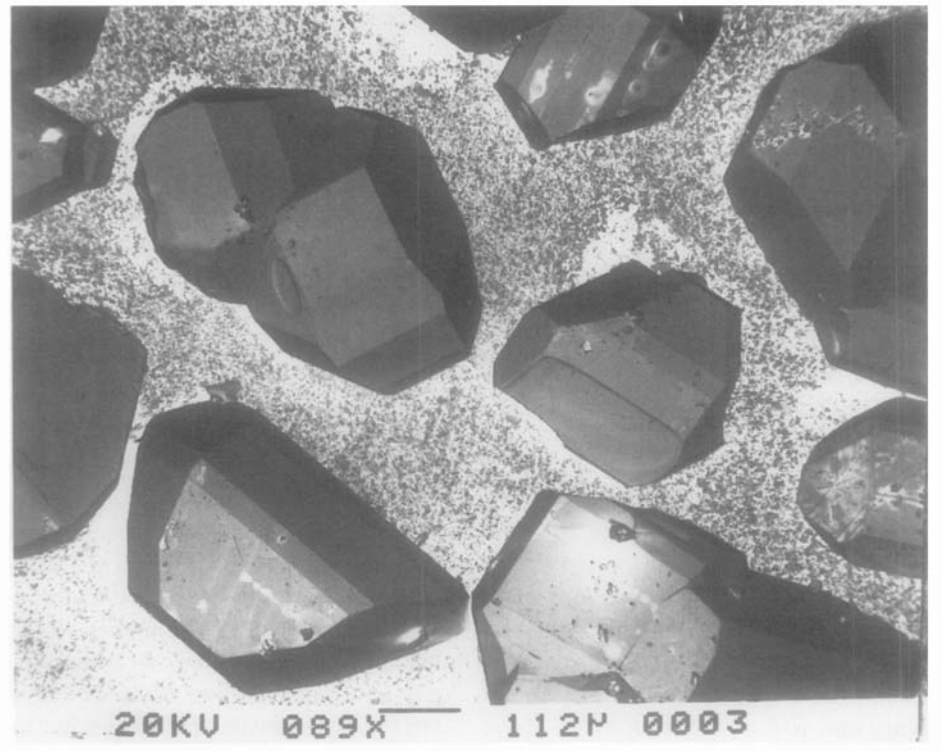

FIG. 1. Scanning electron micrograph showing $AgZnLaP_2$ crystals prepared by recrystallization with iodine at 1000°C. Magnification ×89.

vacuum chamber, connected to a two-stage pump and a helium closed cycle refrigerator, was used to vary the temperature between 20 and 300 K.

Magnetic susceptibilities were determined on CVT recrystallized powders of the new phosphides using a SHE Model 905 SQUID magnetometer at temperatures between 6 and 280 K in fields between 5 and 40 kG. The measured magnetizations were corrected for the diamagnetism of the Kel-F (polychlorotrifluoroethylene) sample container (-6×10^{-4} emu at 6 K, 5 kG).

Diffuse reflectance spectra of microcrystalline powdered samples of the three new phosphides were recorded on a Perkin–Elmer Lambda 9 UV/VIS/NIR spectrophotometer in the 6000–40000 cm^{-1} range.

Results and Discussion

$AgZnLaP_2$, $AgZnSmP_2$, and $CuZnSmP_2$ can be prepared as single phase microcrystalline powders by direct reaction of the elements. All three are gray and have metallic luster. Since these phosphides are hard, have melting points greater than 1100°C, and sinter above 800°C, we classify them as ceramic materials.

Increasing the reaction time occasionally has resulted in the formation of small single crystals, but these were not large enough for X-ray difraction studies. Attempts to recrystallize the prereacted phosphides by iodine chemical vapor transport in a positive temperature gradient (from high temperature to low temperature) invariably resulted in the thermal decomposition of the quaternary phase, due to the higher

TABLE II

WAVELENGTH DISPERSIVE X-RAY ANALYSIS DATA FOR $AgZnLaP_2$, $AgZnSmP_2$, AND $CuZnSmP_2$

Compound	Element	Expected wt%	Measured wt%
$AgZnLaP_2$	Ag	28.83	27.85
	Zn	17.48	17.13
	La	37.13	37.43
	P	16.56	16.67
$AgZnSmP_2$	Ag	27.97	27.35
	Zn	16.96	17.68
	Sm	39.01	38.97
	P	16.06	16.44
$CuZnSmP_2$	Cu	18.62	18.92
	Zn	19.16	19.10
	Sm	44.07	43.37
	P	18.15	18.82

vapor pressure of the zinc volatile species with respect to the other components of the system. On the other hand, transport in a negative temperature gradient did not take place. Isothermal transport with iodine, also called mineralization, has been found to be an adequate method to grow single crystals of the new quaternary phosphides. Growth of 0.1-mm single crystals of the quaternary phosphides required a minimum of 3 days at 1000°C. Best results, in terms of crystallinity, have been obtained for $AgZnLaP_2$. Figure 1 shows an SEM micrograph of some AgZn LaP_2 crystals, in which the three-dimensional nature of the material is evident.

The microprobe data collected for single crystals of $AgZnLaP_2$, $AgZnSmP_2$, and $CuZnSmP_2$ are reported in Table II. The weight percentage observed is typically within 2% of that expected on the basis of the stoichiometric ratios. In addition, the stoichiometry and crystallinity of the final product are not affected by excess phosphorus in the reaction mixture. We conclude that the stoichiometries do not deviate significantly from 1:1:1:2.

TABLE III

CRYSTAL PARAMETERS OF $AgZnSmP_2$ at 25°C[a,b]

$a = b = 4.1247(4)$ Å
$c = 6.6920(6)$ Å
$a = \beta = 90°$
$\gamma = 120°$
$V = 98.60(3)$ Å^3
Space group: $P\bar{3}m1$
Formula weight = 385.5 amu
$Z = 1$
d(calc) = 6.49 g · cm^{-3}
μ (calc) = 264.0 cm^{-1}

[a] Unit cell parameters and their e.s.d.'s were derived by a least-squares fit to the setting angles of the unresolved Mo$K\alpha$ components of 24 reflections with 2θ between 32° and 36°.

[b] In this and all subsequent tables the e.s.d.'s of all parameters are given in parameters, right-justified to the least significant digit(s) of the reported value.

$AgZnSmP_2$ has trigonal symmetry. The final cell parameters are summarized in Table III. The positional and thermal parameters of the atoms are given in Tables IV and V, respectively. Table VI shows the interatomic distances and coordination numbers. The structure consists of a hexagonal array of phosphorus atoms with the samarium atoms occupying half of the octa-

TABLE IV

POSITIONAL PARAMETERS AND THEIR ESTIMATED STANDARD DEVIATIONS FOR $AgZnSmP_2$

Atom	x	y	z	B(Å^2)
Sm	0.000	0.000	0.000	0.584(5)
Ag	0.333	0.667	0.3666(1)	0.938(6)
Zn	0.333	0.667	0.367	0.938
P	0.333	0.667	0.7541(2)	0.73(2)

Note. The thermal parameter given is the isotropic equivalent thermal parameter defined as: (4/3) $*[a^2*\beta(1,1) + b^2*\beta(2,2) + c^2*\beta(3,3) + ab(\cos\gamma)*\beta(1,2) + ac(\cos\beta)*\beta(1,3) + bc(\cos\alpha)*\beta(2,3)]$, where a, b, c are real cell parameters, and $\beta(i, j)$ are anisotropic betas.

TABLE V

ANISOTROPIC THERMAL PARAMETERS FOR $AgZnSmP_2$[a]

Atom	$B(1,1)$	$B(2,2)$	$B(3,3)$	$B(1,2)$	$B(1,3)$	$B(2,3)$	B_{eqv}
Sm	0.632(8)	$B(1,1)$	0.49(1)	$B(1,1)$	0	0	0.584(5)
Ag	1.09(1)	$B(1,1)$	0.62(1)	$B(1,1)$	0	0	0.938(6)
Zn	(Restrained to identity with Ag)				0	0	0.938
				$B(1,1)$			
P	0.85(4)	$B(1,1)$	0.48(5)	$B(1,1)$	0	0	0.73(2)

[a] The form of the anisotropic temperature factor is: $\exp[-1/4\{h2a^*2B(1,1) + k2b^*2B(2,2) + l2c^*2B(3,3) + 2hka^*b^*B(1,2) + 2hla^*c^*B(1,3) + 2klb^*c^*B(2,3)\}]$, where a^*, b^*, and c^* are reciprocal lattice constants.

hedral holes and the silver and zinc atoms occupying half of the tetrahedral holes. The Sm atoms lie in planes at $z = 0, 1$, the P atoms in planes at $z = 0.246, 0.754$, and the Zn and Ag atoms in a pair of planes at $z = 0.5 \pm 0.1333$. This view is shown in Fig. 2.

All atoms reside on special positions in the space group. The P–P distances are almost identical within (4.125 Å) and between the layers (4.063 and 4.152 Å). The alternate interplanar spacings of the phosphorus layers are 3.291 (narrow) and 3.401 Å (wide). The structure is ordered such that, with the phosphorus layers labeled A–B–A–B . . . , the silver and zinc atoms occupy all the tetrahedral holes in the A–B (wide) interlayers and the samarium atoms occupy all the octahedral holes in the B–A (narrow) interlayers. The occupancy of the tetrahedral holes by silver and zinc appears to be random with no evidence of long range order. There is no indication of significant occupation of the alternate octahedral and tetrahedral sites in the crystal; the empty sites show no significant residual electron density.

TABLE VI

INTERATOMIC DISTANCES AND COORDINATION NUMBERS IN $AgZnSmP_2$

Atom 1	Atom 2	Distance (Å)	Coordination number
Sm	P	2.895(1)	6
Sm	Ag/Zn	3.419(1)	6
Ag/Zn	P(eq)	2.515(1)	3
Ag/Zn	P(ax)	2.593(2)	1
Ag/Zn	Ag/Zn	2.976(1)	3
Ag/Zn	Sm	3.419(1)	3
P	P	4.125(1)[a]	6
P	P	4.063(3)	3
P	P	4.152(3)	3
P	Sm	2.895(1)	3
P(eq)	Ag/Zn	2.515(1)	3
P(ax)	Ag/Zn	2.593(2)	1

[a] Translation by a or b axis.

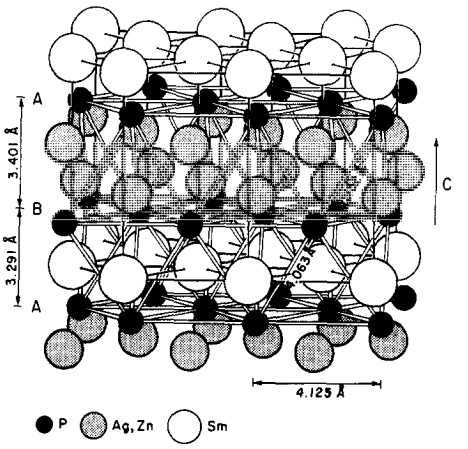

FIG. 2. ORTEP drawing of the crystal structure of $AgZnSmP_2$ along the c axis. A segment, approximately 12 × 12 × 7 Å, is shown. The phosphorus atoms are packed hexagonally. The holes between the phosphorus layers are occupied alternately by Sm (in half the octahedral holes) or by Ag and Zn (in half the tetrahedral holes).

Due to the disorder, the Ag and Zn atomic positions and thermal parameters were constrained to be identical. All distances have e.s.d.'s which are too small by an amount equivalent to the e.s.d. of the cell dimensions involved. This error in the e.s.d. is small, and all the e.s.d.'s certainly underestimate the variability of the distances; the rms thermal motion is larger than the e.s.d. of the bond distances. No bond error smaller than 0.001 has been quoted.

It is interesting to note that the structure of $AgZnSmP_2$ is a derivative of the NiAs-type structure. In NiAs, the As atoms are in a hexagonal close-packed array with Ni atoms in all of the octahedral holes. While the Sm atoms occupy the same positions as Ni in NiAs, the z coordinates of the Ag/Zn atoms have shifted from 0.5 ± 0.125 (3/8 and 5/8) to 0.5 ± 0.1333. The P atoms at $z = 0.246, 0.754$ are nearly identical in position to the As atoms at $z = 1/4, 3/4$.

$AgZnLaP_2$ and $CuZnSmP_2$ are isostructural with $AgZnSmP_2$. Cell parameters determined from single crystal photographs are $a = 4.19 \pm 0.02$ Å, $c = 6.82 \pm$ Å for $AgZnLaP_2$ and $a = 4.00 \pm 0.02$ Å, $c = 6.59 \pm 0.02$ Å for $CuZnSmP_2$. The indexed powder patterns for these compounds are given in Tables VII and VIII. The cell parameters obtained from these patterns are $a = 4.194 \pm 0.002$ Å, $c = 6.817 \pm 0.002$ Å for $AgZnLaP_2$ and $a = 4.016 \pm 0.002$ Å, $c = 6.592 \pm 0.002$ Å for $CuZnSmP_2$.

A preliminary determination of the temperature dependences of the electrical resistivities of $CuZnSmP_2$, $AgZnSmP_2$, and $AgZnLaP_2$ obtained from sintered pellets are shown in Fig. 3. The data were found to be reproducible for repeated heating and cooling cycles. The specific resistivity values for all four compounds are in the 0.1–0.2 Ω-cm range, which is an indication that these materials are small band gap semiconductors. No appreciable temperature dependence is observed in any of the samples in the extrinsic region, even at low temperatures. At temperatures above approximately 100 K, the resistivity variation of $AgZnSmP_2$ and $CuZnSmP_2$ is much like that of a metal (increases with increasing temperature). This type of behavior is characteristic of heavily doped (degenerate) semiconductors. On the other hand, $AgZnLaP_2$

TABLE VII

POWDER DIFFRACTION PATTERN OF $AgZnLaP_2$

$h\ k\ l$	I/I_1	d_o (Å)	d^c (Å)
0 1 1	vs	3.2065	3.2056
0 1 2	vs	2.4852	2.4855
0 0 3	w	2.2722	2.2725
1 1 0	vs	2.0968	2.0970
0 1 3	m	1.9263	1.9265
0 2 1	m	1.7548	1.7549
0 2 2	m	1.6023	1.6028
0 1 4	vs	1.5429	1.5429
0 2 3	w	1.4189	1.4187
1 2 1	m	1.3461	1.3458
0 1 5	s	1.2762	1.2765
0 2 4	w	1.2440	1.2428
0 3 0	w	1.2110	1.2107
1 2 3	w	1.1753	1.1751
1 1 5	w	1.1430	1.1431
0 2 5	vw	1.0911	1.0904
0 1 6	vw	1.0846	1.0844
1 2 4	s	1.0695	1.0692
2 2 0	m	1.0487	1.0485
1 1 6	m	0.9985	0.9990
1 2 5	s	0.9677	0.9674
2 2 3	w	0.9526	0.9521
1 3 3	vw	0.9208	0.9209
0 4 0	vw	0.9078	0.9080
0 4 1	vw	0.9004	0.9001
0 4 2	w	0.8776	0.8775
1 2 6	vw	0.8750	0.8753
2 3 0	vw	0.8331	0.8332
0 1 8	w	0.8294	0.8296
0 3 6	w	0.8287	0.8285
2 3 2	vw	0.8095	0.8094
1 2 7	vw	0.7941	0.7943
1 4 0	vw	0.7923	0.7926
1 1 8	w	0.7896	0.7895
2 3 3	vw	0.7825	0.7824

Note. Trigonal, space group $P\bar{3}m1$, $a = 4.194 \pm 0.002$ Å, $c = 6.817 \pm 0.002$ Å. Ni-filtered Cu radiation $\lambda\alpha_1 = 1.5405$ Å. Debye–Scherrer camera diameter = 11.46 cm.

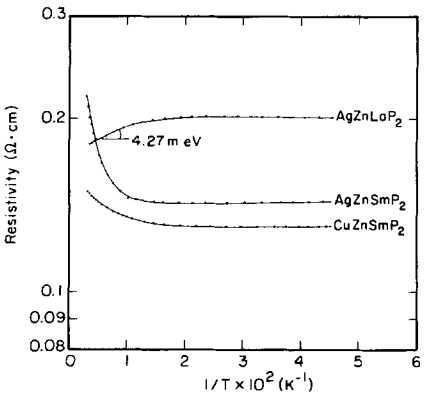

FIG. 3. Resistivity vs temperature for $AgZnLaP_2$, $AgZnSmP_2$, and $CuZnSmP_2$. The specific resistivity values for all three samples indicate semiconducting behavior.

exhibits typical semiconductor behavior at high temperatures (resistivity decreases with increasing temperature).

The magnetic susceptibilities of $AgZnSmP_2$ and $AgZnLaP_2$ were measured as a function of temperature. $AgZnLaP_2$ is diamagnetic, and the magnetic susceptibility shows only a very small temperature dependence, as is characteristic of diamagnetic semiconductors. The magnetic susceptibility of $AgZnSmP_2$, on the other hand, is paramagnetic due to the localized *f*-electrons on Sm^{3+}, and temperature dependent.

The diffuse reflectance spectra of $AgZnLaP_2$, $AgZnSmP_2$, and $CuZnSmP_2$ are shown in Fig. 4. An energy gap of 0.12 eV for $AgZnLaP_2$ has been deduced from the reflectance step observed in the low energy region of the spectrum. It should be noted here that the absorption edge occurs, in general, at higher energies (about 0.04 eV on average) compared with the corresponding reflection edge (*9*). In contrast with $AgZnLaP_2$, the step in reflectance is not resolved in the spectra of $AgZnSmP_2$ and $CuZnSmP_2$, presumably due to the higher doping levels present in these materials. With increased doping the conduction band edge is expected to shift uniformly downward, and the valence band edge uniformly upward, causing the energy gap to decrease in proportion to the dopant concentration.

Another feature characteristic of the

TABLE VIII

POWDER DIFFRACTION PATTERN OF $CuZnSmP_2$

h k l	I/I_1	d_o (Å)	d_c (Å)
0 1 1	vs	3.0767	3.0761
0 1 2	vs	2.3928	2.3924
0 0 3	w	2.1981	2.1975
1 1 0	vs	2.0075	2.0080
0 1 3	w	1.8578	1.8577
0 2 1	m	1.6813	1.6815
0 2 2	m	1.5376	1.5380
0 1 4	s	1.4858	1.4893
1 1 3			1.4823
0 2 3	w	1.3640	1.3636
1 2 1	m	1.2892	1.2892
0 1 5	w	1.2324	1.2328
1 2 2	m	1.2208	1.2210
0 2 4	vw	1.1960	1.1962
0 3 0	vw	1.1587	1.1593
1 2 3	vw	1.1281	1.1281
1 1 5	vw	1.1015	1.1021
0 1 6	w	1.0473	1.0476
0 3 3	m	1.0251	1.0253
2 2 0	w	1.0033	1.0040
1 3 1	w	0.9542	0.9544
0 2 6	w	0.9291	0.9289
1 3 2	w	0.9258	0.9258
2 2 3	w	0.9132	0.9132
0 1 7	vw	0.9092	0.9090
1 3 3	vw	0.8831	0.8833
0 3 5	vw	0.8706	0.8706
0 4 1	vw	0.8620	0.8620
1 2 6	w	0.8430	0.8430
0 4 2	w	0.8407	0.8407
1 3 4	w	0.8325	0.8325
0 2 7	vw	0.8280	0.8281
0 0 8	vw	0.8240	0.8240
0 4 3	vw	0.8085	0.8085
2 2 5	vw	0.7987	0.7987
2 3 1	m	0.7922	0.7921
1 3 5	m	0.7785	0.7785
2 3 2	m	0.7755	0.7755

Note. Trigonal, space group $P\bar{3}m1$, $a = 4.016 \pm 0.002$ Å, $c = 6.592 \pm 0.002$ Å. Ni-filtered Cu radiation $\lambda\alpha_1 = 1.5405$ Å. Debye–Scherrer camera diameter = 11.46 cm.

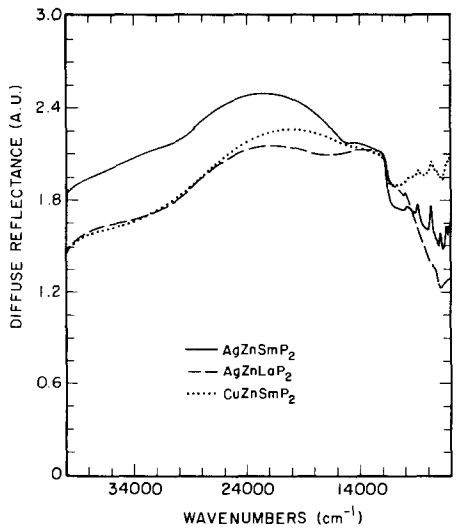

FIG. 4. Diffuse reflectance spectra of $AgZnLaP_2$, $AgZnSmP_2$, and $CuZnSmP_2$. An energy gap of 0.12 eV is obtained for $AgZnLaP_2$. The reflection edge is not resolved in the spectra of $AgZnSmP_2$ and $CuZnSmP_2$ due to heavy doping and overlap with the bands due to Sm(III) f–f transitions. (*Note:* The sharp change in reflectance at 11670 cm^{-1} is due to a detector change.)

spectra of $AgZnSmP_2$ and $CuZnSmP_2$ is the series of sharp lines observed in the 6000–9000 cm^{-1} region. These bands correspond to f–f transitions from the Sm(III) ground-state $^6H_{5/2}$ to $^6F_{1/2}$ (6200 cm^{-1}), $^6H_{15/2}$ (6350 cm^{-1}), $^6F_{3/2}$ (6450 cm^{-1}), $^6F_{5/2}$ (7000 cm^{-1}), $^6F_{7/2}$ (7840 cm^{-1}), and $^6F_{9/2}$ (9000 cm^{-1}).

Conclusions

$AgZnLaP_2$, $AgZnSmP_2$, and $CuZnSmP_2$ are a new class of phosphides with a three-dimensional structure consisting of hexagonally packed layers of P^{3-}. The Ag^+ (or Cu^+) and Zn^{2+} ions occupy half of the tetrahedral holes and Sm^{3+} (or La^{3+}) ions half of the octahedral holes. We note that we expect that other rare-earth ions can be substituted for La and Sm, particularly rare-earth ions whose size is between that of La and Sm. We are not sure how small the rare-earth ion can be except to note that $AgZnYP_2$ does not form; a new ternary compound Ag_3YP_2 forms instead.

Preliminary evidence suggests that these quaternary phosphides are quite stable; these compounds do not react with water at room temperature, and do not decompose in air upon heating to 700°C. Furthermore, because these phosphides sinter near 800°C and are relatively hard, we feel that they should be classified as new ceramics.

Electrical measurements indicate that these materials are degenerate semiconductors. Since impurities were not detected with microprobe analysis, the doping levels are probably quite small. Likely impurities include silicon and oxygen from the quartz reaction ampoules. The fact that the materials are grey indicates that the band gap must be less than about 1.8 eV. Until undoped single crystals suitable for measurements of infrared transmittance can be prepared, it is not possible to tell whether these materials have a window in the infrared.

It is interesting to note that the diffuse reflectance spectra show that the band gap of doped $AgZnLaP_2$ is the largest and that of doped $CuZnSmP_2$ the smallest. We suggest that there may be a correlation with unit cell volume; the larger the volume, the larger the band gap. Perhaps phosphides with larger cations will have band gaps in the visible region.

Acknowledgments

The crystal structure analysis was performed by Dr. F. J. Hollander, staff crystallographer at the U.C. Berkeley X-Ray Crystallographic Facility (CHEXRAY). The authors thank R. Schwartz and T. A. Vanderah for many useful discussions, and J. Donovan for help with the microprobe analysis. This research was supported by the Office of Naval Research (Contract N00014-87-0660). Financial support for P. T. from the Consejo Superior de Investigaciones Cientificas, Madrid is gratefully acknowledged. A.M.S. thanks the

Alfred P. Sloan Foundation and the Camille and Henry Dreyfus Foundation for their support.

References

1. A. E. BENCE AND A. L. ALBEE, *J. Geol.* **78,** 382 (1968).
2. University of California, Berkeley Chemistry Department X-Ray Crystallographic Facility (CHEX-RAY). Enraf-Nonius software as described in the CAD4 operation manual, Enraf-Nonius, Delft, Nov. 1977, updated Jan. 1980.
3. Structure determination Package User's Guide, B. A. Frenz and Associates, Inc., College Station, Texas (1985).
4. W. H. ZACHARIASEN, *Acta Crystallogr.* **16,** 1139 (1963).
5. D. T. CROMER AND J. T. WABER, "International Tables for X-Ray Crystallography," Vol. IV, Table 2.2B, The Kynoch Press, Birmingham, England, (1974).
6. D. T. CROMER AND J. T. WABER, "International Tables for X-Ray Crystallography," Vol. IV, Table 2.3.1, The Kynoch Press, Birmingham, England (1974).
7. M. E. STRAUMANIS, *J. Appl. Phys.* **20,** 726 (1949).
8. M. U. COHEN, *Rev. Sci. Instrum.* **6,** 68 (1935); **7,** 155 (1936).
9. M. CARDONA AND G. HARBEKE, *J. Appl. Phys.* **34,** 813 (1963).